Evolution of the Magnetic Excitations in NaOsO$_3$ through its Metal-Insulator Transition

J. G. Vale,[1,2,*] S. Calder,[3,†] C. Donnerer,[1] D. Pincini,[1,4] Y. G. Shi,[5,6] Y. Tsujimoto,[6] K. Yamaura,[6,7] M. Moretti Sala,[8]
J. van den Brink,[9] A. D. Christianson,[3,10] and D. F. McMorrow[1]

[1]*London Centre for Nanotechnology and Department of Physics and Astronomy,*
University College London, Gower Street, London WC1E 6BT, United Kingdom
[2]*Laboratory for Quantum Magnetism, École Polytechnique Fédérale de Lausanne (EPFL), Lausanne CH-1015, Switzerland*
[3]*Neutron Scattering Division, Oak Ridge National Laboratory, Oak Ridge, Tennessee 37831, USA*
[4]*Diamond Light Source, Harwell Science and Innovation Campus, Didcot, Oxfordshire OX11 0DE, United Kingdom*
[5]*Beijing National Laboratory for Condensed Matter Physics and Institute of Physics,*
Chinese Academy of Sciences, Beijing 100190, China
[6]*Research Center for Functional Materials, National Institute for Materials Science, 1-1 Namiki, Tsukuba, Ibaraki 305-0044, Japan*
[7]*Graduate School of Chemical Sciences and Engineering, Hokkaido University,*
North 10 West 8, Kita-ku, Sapporo, Hokkaido 060-0810, Japan
[8]*ESRF, The European Synchrotron, 71 Avenue des Martyrs, 38043 Grenoble, France*
[9]*Institute for Theoretical Solid State Physics, IFW Dresden, D01171 Dresden, Germany*
[10]*Department of Physics and Astronomy, University of Tennessee, Knoxville, Tennessee 37996, USA*

The temperature dependence of the excitation spectrum in NaOsO$_3$ through its metal-to-insulator transition (MIT) at 410 K has been investigated using resonant inelastic x-ray scattering at the Os L_3 edge. High-resolution ($\Delta E \sim 56$ meV) measurements show that the well-defined, low-energy magnons in the insulating state weaken and dampen upon approaching the metallic state. Concomitantly, a broad continuum of excitations develops which is well described by the magnetic fluctuations of a nearly antiferromagnetic Fermi liquid. By revealing the continuous evolution of the magnetic quasiparticle spectrum as it changes its character from itinerant to localized, our results provide unprecedented insight into the nature of the MIT in NaOsO$_3$ [J. G. Vale, S. Calder, C. Donnerer, D. Pincini, Y. G. Shi, Y. Tsujimoto, K. Yamaura, M. M. Sala, J. van den Brink, A. D. Christianson, and D. F. McMorrow, Phys. Rev. B **97**, 184429 (2018)].

The nature of the metal-to-insulator transition (MIT) in transition metal oxides (TMOs) is of enduring interest, as it represents a spectacular manifestation of competing interactions and their effects on the most fundamental transport property of materials. Recently, considerable attention has focused on the nature of the MIT in 5d TMOs, which have the additional ingredients of strong spin-orbit coupling and a lower degree of localization relative to their 3d counterparts [1,2]. New phenomenology has been revealed by experiments, including a number of MITs which are intimately entwined with the onset of magnetic order. Notably, these MITs do not appear to be associated with any spontaneous lattice symmetry breaking, placing them outside of the conventional Mott-Hubbard paradigm. A key and yet unsolved issue for such systems is to fully determine the nature of the magnetic quasiparticle spectrum as the electronic character evolves from itinerant to localized through the MIT.

The classification of magnetic interactions between full itinerancy and localization is usually described in one of two limits [3]. In the local moment (Heisenberg) limit, magnetism in insulators is assumed to arise from unpaired electrons within an atomic picture. At some temperature T, the orientation of the magnetic moments varies, but their magnitude remains fixed at the $T = 0$ value. Consequently, only the transverse component of the local spin-density fluctuation (LSF) $\chi^{\pm}(q, \omega)$ is important. This gives rise to collective spin-wave excitations and is generally applicable to magnetic insulators. At the other extreme (itinerant or Stoner limit), the electrons and spin fluctuations are extended in real space, with thermodynamic properties of the system governed by intraband electron-hole pair interactions, which have a degree of collective behavior. At some temperature T, the orientation of the magnetic moments remains fixed, but their magnitude is reduced from the $T = 0$ value. In this limit, the longitudinal component $\chi^{zz}(q, \omega)$ and the temperature dependence of the LSF are important. Between these two limits, one typically observes Landau damping of spin waves by intraband particle-hole excitations. Damping is more prevalent at large wave vectors q, since there are a greater number of available states for the corresponding magnon to decay into. Such an effect has been observed in a number of materials, notably, doped La$_{2-x}$Sr$_x$CuO$_4$ [4–6] and a subset
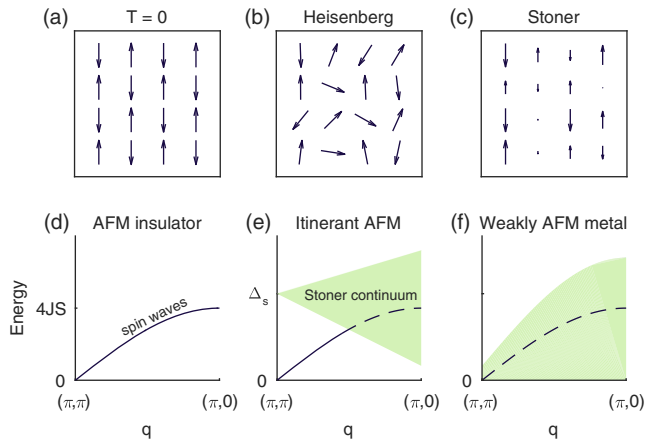
FIG. 1. Top panels: Schematic of the orientation of antiferro-magnetically (AFM) interacting magnetic moments on a square lattice for $T = 0$ and finite temperatures in the Heisenberg or Stoner limits. Bottom panels: Excitation spectra in the Heisenberg limit, for an itinerant AFM (with critical energy scale Δ_s) and for a metal with weak AFM correlations. Dashed lines indicate damped excitations.

of the iron pnictides [7–12]. A summary of the behavior in the respective limits is shown schematically in Fig. 1.

Here we focus our attention upon materials which undergo continuous MITs with temperature, that are concomitant with the onset of long-ranged, commensurate antiferromagnetic order. Moreover, the crystallographic space group remains constant through the MIT. Examples include some of the $5d^5$ pyrochlore iridates $R_2Ir_2O_7$ ($R = Ln^{3+}$) [13,14], plus the $5d^3$ osmates $Cd_2Os_2O_7$ [15–17] and $NaOsO_3$. The latter material has been proposed to be an example of a Slater insulator [18–22], in which the formation of antiferromagnetic order itself at $T_{MI} = 410$ K drives the formation of an insulating gap below the Néel temperature. This interpretation, however, is not universally accepted [23]. Nevertheless, together with significant spin-phonon coupling [24], one observes an unprecedented connection between the magnetic, electronic, structural, and phonon degrees of freedom in $NaOsO_3$.

One would thus expect the electronic and magnetic excitations to evolve correspondingly through the MIT. Optical conductivity measurements on $NaOsO_3$ reveal a continuous opening of the electronic gap with a decreasing temperature $\{\Delta_g(0) = 102(3)$ meV$\}$ [22] and an MIT in which electronic correlations play a limited role. This is consistent with a Slater picture in which interactions are mean-field-like. Meanwhile, previous resonant inelastic x-ray scattering (RIXS) measurements showed well-defined and strongly gapped (~ 50 meV) dispersive spin-wave excitations at 300 K [25]. This was found to be consistent with an anisotropic nearest-neighbor Heisenberg picture for the magnetic Hamiltonian and is suggestive of localized magnetic moments. The question remains whether either the spin or electronic excitations remain coherent through

the MIT and if there is any evidence of coupling to any of the other relevant degrees of freedom present in the system.

In this Letter (and Ref. [26]), we establish that there is a continuous progression from itinerant to localized behavior through the MIT in $NaOsO_3$. This is revealed by a significant renormalization of the magnetic quasiparticle spectral weight over large ranges of momentum and energy. In particular, the presence of correlations in the metallic state immediately leads to a deviation from mean-field behavior and, hence, true Slater phenomenology.

Our experiments relied on exploiting the unique ability of RIXS to provide momentum-resolved sensitivity to the excitations of the orbital, electronic, and magnetic degrees of freedom. By providing data on an experimental test case, in which the magnetic quasiparticle spectrum can be tuned simply by varying the temperature, our work in turn helps extend the utility of RIXS, which has hitherto been best understood in the localized limit [27–29].

RIXS measurements were performed at the Os L_3 edge [36] ($E = 10.877$ keV, $2p \rightarrow 5d$) on the ID20 spectrometer at the ESRF, Grenoble. Preliminary measurements were performed at 9-ID-B, Advanced Photon Source. The energy resolution of the spectrometer was estimated to be $\Delta E = 56$ meV, based upon scattering from transparent adhesive tape. The incident energy used equates to 3 eV below the maximum of the white line obtained from x-ray absorption spectroscopy. Further experimental details are provided in Ref. [26].

Our initial measurements focused upon the high-energy orbital excitations from the ground state (intra-t_{2g} and $t_{2g} \rightarrow e_g$), which were consistent with those observed in Ref. [25]. We were unable to determine any significant temperature dependence of these broad excitations. This corroborates the supposition that the MIT is not driven by local structural distortion, which would manifest in significant variations of the local crystal field parameters.

The main focus of this Letter is the low-energy excitation spectrum below 0.5 eV. RIXS spectra were collected at three different momentum transfers as a function of the temperature: Γ (4.95, 2.95, 3.95), Γ-Y (5, 2.75, 4), and Y (5, 2.5, 4). This reflects a progression from the Brillouin zone center to the zone boundary. Note that $NaOsO_3$ exhibits $Q_{AFM} = 0$ order; that is, the structural and magnetic lattices are commensurate with one another. Hence, the point near Γ was chosen in order to avoid the weak magnetic Bragg peak at (5, 3, 4). Four RIXS spectra were collected for each temperature and momentum transfer (30 s/pt). These spectra were each normalized to the intensity of the intra-t_{2g} excitations at 1 eV energy loss, cross-correlated to account for any temporal shift in the elastic line position, and then averaged.

Representative RIXS spectra (at Γ-Y) are plotted in Fig. 2(a), for temperatures below and above the MIT [30]. They are also shown with the elastic line and d-d contributions subtracted [Figs. 2(b)], in order to better
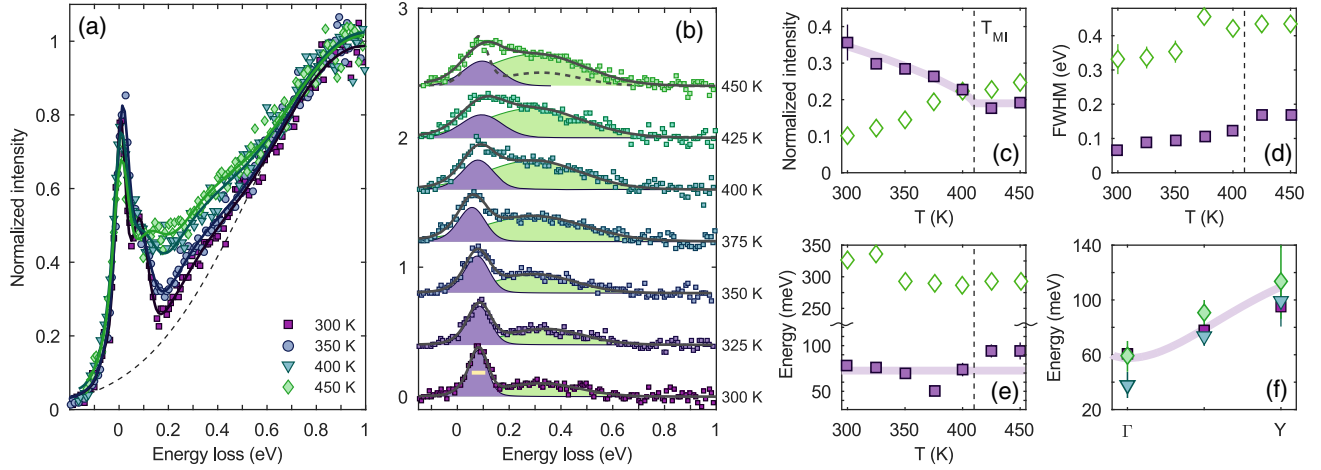
FIG. 2. Analysis of RIXS spectra collected at Γ-Y. (a) Representative low-energy RIXS spectra, each of which is normalized to the d-d excitations at 1 eV energy loss (dashed line). (b) Spectra with the elastic line and d-d contributions subtracted off. Added are the best fit to the data (black solid line) and relative components of the magnon peak (purple) and high-energy continuum (green). The dashed line superimposed on 450 K plot is the best fit to 300 K data for comparison. The yellow bar indicates the FWHM of the resolution function. (c)–(e) Fitted peak intensity (c), intrinsic FWHM (d), and energy (e) of the magnon peak (filled squares) and high-energy continuum (open diamonds) as a function of the temperature. Solid lines are guides to the eye. (f) Energy of the magnon peak as a function of the momentum transfer and temperature. The symbols are the same as (a). The solid line is the best fit to dispersion at 300 K as determined within Ref. [25].

isolate changes to the spectra below 1 eV. The spectrum at 300 K is in agreement with that given in Ref. [25], with a sharp dispersive peak evident at 60–100 meV energy loss attributable to a single magnon excitation. This peak progressively weakens and broadens with increasing temperature. Strikingly, concurrent with the diminishing of the single magnon peak, there is a continuous increase in the intensity between 0.1 and 0.6 eV, while there is no significant change in the intra-t_{2g} excitations.

In order to quantify these observations further, the data were fitted with Gaussians to represent the elastic line, magnon peak, broad component centered around 300 meV, and the intra-t_{2g} excitations. The fits in the low-energy portion of the RIXS spectra were corrected to take the Bose factor into account. Prior to fitting, the model line shape was convoluted with the (asymmetric) experimental resolution function [26]. This minimal model for the line shape was used in order to reduce the number of free parameters in the fit while allowing the relevant features of the data to be captured. The results of these fits are given in the remaining panels in Fig. 2. Our simple model gives a good description of the experimental data, with $0.8 \leq \chi^2/\nu \leq 1.3$ for all data sets. Clearly, there is a significant variation of the RIXS spectra through the MIT, as $NaOsO_3$ progresses from the localized to the itinerant limit. We briefly discuss the temperature dependence of the fitted parameters.

First, the peak at 80 meV appears to weaken progressively with an increasing temperature for all momentum transfers [Fig. 2(c)]. This abates at T_N, with some residual intensity remaining all the way to 450 K, and confirms its previous assignment as a magnon peak [25]. Second, the

energy of the magnon peak appears to weakly vary with temperature [Fig. 2(e)]. However, the magnon dispersion at 450 K appears remarkably similar to that collected at 300 K [within experimental uncertainty, Fig. 2(f)]. We note that the previously reported value for the effective uniaxial anisotropy [$\Gamma = 1.4(1)$ meV] is likely to be an overestimate of the true magnitude. This is due to the effect of the finite momentum resolution of the RIXS spectrometer, which was not taken into account within the minimal model presented in Ref. [25]. Combined with the finite energy resolution, this means that any temperature dependence of the spin gap is likely to be washed out and difficult to observe.

Finally, the width of the magnon peak increases as a function of the increasing temperature for all momentum transfers [Fig. 2(d)]. In Ref. [25], it was proposed that the well-defined, resolution-limited spin-wave excitations at 300 K were evidence of localized (Heisenberg) behavior. Yet, with the aid of our new fitting model, we observe experimentally that the magnons have an intrinsic FWHM of 30 meV at Γ, increasing to 70 meV at larger momentum transfers [26]. Some of this damping may arise from processes known to apply in the localized limit (four-magnon, magnon-phonon coupling). There is, however, the omnipresent continuous MIT at 410 K. Previous bulk measurements have shown that the charge gap $\Delta_g \sim$ 80 meV at 300 K [18], with the optical gap having a similar magnitude [22]. Within a weak coupling theory, collective antiferromagnetic spin-wave excitations are expected to merge into a Stoner continuum above a critical energy Δ_s [Fig. 1(e)]. By using theoretical expressions
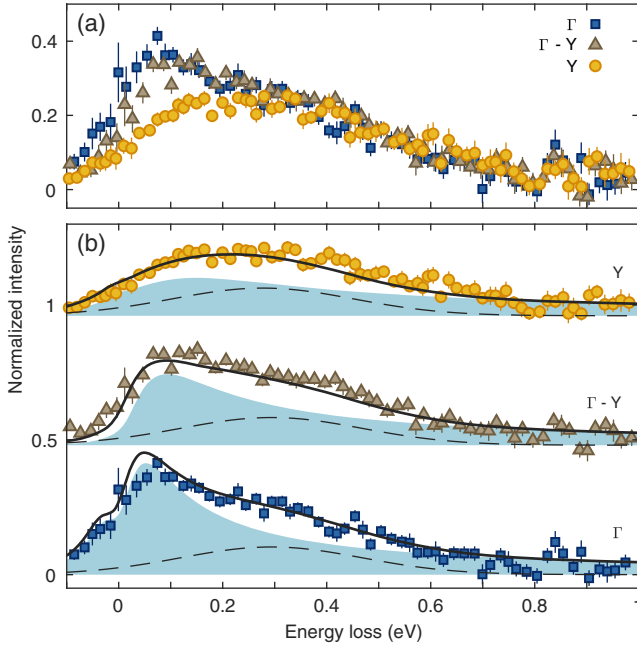
FIG. 3. Paramagnetic spin fluctuations (SFs) in NaOsO$_3$ at 450 K. (a) Experimental data collected at various crystal momenta. For clarity, the elastic line and high-energy intra-t_{2g} excitations have been subtracted. (b) Comparison of the WAFL model (solid line) with experimental data. The filled area indicates the paramagnetic SF calculated using Eq. (1), with $\gamma = 0.02$ meV^{-1} and $\xi/a_0 \sim 1$. The dashed line is a momentum-independent high-energy contribution, which likely results from interband particle-hole excitations.

given within Ref. [31], we find that $\Delta_s \sim 60$ meV for NaOsO$_3$ [26], implying that the magnons are (weakly) Landau damped for all wave vectors.

Here we focus on the characteristics of the RIXS spectrum in the metallic phase at 450 K and what the magnetic quasiparticle spectrum reveals about the nature of the electronic state of the metallic phase. (A detailed discussion of the low-energy magnetic excitations deep in the insulating antiferromagnetic phase can be found in Ref. [25].)

The RIXS spectra are plotted in Fig. 3(a); the elastic and intra-t_{2g} contributions have been subtracted in order to highlight the salient features. A broad asymmetric feature can be observed, the shape and amplitude of which varies with the momentum transfer. Meanwhile, the high-energy portion (> 0.3 eV) appears momentum *independent*. The simple underdamped fitting model used in Fig. 2 leads to somewhat ambiguous results above T_N; this is especially the case for higher momentum transfers where the excitations are weaker [26]. We therefore considered models which more naturally describe spin fluctuations in the metallic phase, noting that previous bulk measurements [18] suggest NaOsO$_3$ exhibits paramagnetic Fermi liquid behavior above the Néel temperature.

Specifically, we used the self-consistent renormalization theory appropriate for a weakly antiferromagnetic Fermi liquid (WAFL) [3]. In this picture, magnetic order is destroyed by thermal excitations of long-wavelength spin fluctuations. Yet, even though long-ranged order disappears at T_N, there may be persistent short-ranged antiferromagnetic correlations, which are characterized by some correlation length ξ. These localized clusters of antiferromagnetic order are able to diffuse through the crystal lattice, giving rise to incoherent spin excitations.

For simplicity, we assume that the fluctuations are spatially isotropic and consider a pseudocubic unit cell, with a lattice constant $a_0 = 3.80$ Å given by the Os-Os distance. Following the approach of Inosov and Tucker [32,33], the imaginary part of the dynamic susceptibility $\chi''(\mathbf{Q}, E)$ is given by

$$\chi''(\mathbf{Q}, E) \propto \frac{\chi_0 \Gamma E}{E^2 + \Gamma^2 [1 + \xi^2 (\mathbf{Q} - \mathbf{Q}_{\text{AFM}})^2]^2}. \quad (1)$$

In this expression, the spin relaxation rate Γ is defined through $\Gamma \equiv a_0^2/\gamma \xi^2$, where γ denotes the damping coefficient arising from a spin decay into particle-hole excitations (related to the electronic band structure) and ξ is the spin-spin correlation length. Meanwhile, χ_0 is the staggered susceptibility at $\mathbf{Q}_{\text{AFM}} = 0$ [34]. All of these parameters are, in principle, dependent upon the temperature. For completeness, the anti-Stokes (energy gain) process has also been included; this is a factor of $\exp(-\hbar\omega/kT)$ weaker than the equivalent Stokes (energy loss) process.

There is remarkable agreement between this model for the spin fluctuations and the data [Fig. 3(b)], with the best global fit to the data using $\gamma \sim 0.02$ meV^{-1} and $\xi/a_0 \sim 1$. The magnitude of γ is similar to that found in overdoped Ba(Fe$_{1-x}$Co$_x$)$_2$As$_2$ [33], indicative of itinerant behavior. Moreover, the fact that ξ is on the order of a_0 implies that the spin fluctuations at 450 K are short ranged and that the system is close to the hydrodynamic limit.

We make the following comments. The experimental RIXS cross section includes a number of additional contributions, which include momentum-dependent absorption and polarization effects. This explains the use of a proportionality in Eq. (1), in order to model these contributions phenomenologically. Second, the quantitative agreement with the data was improved through the inclusion of an additional scattering component centered at 0.3 eV [dashed line in Fig. 3(b)]. This component was constrained to be momentum independent, in order to facilitate convergence. The nature of this component is unclear directly from the data. This is because RIXS is sensitive to both electronic and magnetic interactions, and it is difficult to distinguish them *a priori* without further information. We posit that it results primarily from interband particle-hole excitations, based on calculations presented within Ref. [26].

Finally, the fits presented in Fig. 3(b) explicitly use the same scale factor for all momentum transfers, in order to remove any ambiguity related to the proportionality in Eq. (1). The fact that the WAFL model describes the experimental data so well at 450 K, without the use of arbitrary scale factors, is further evidence that this better reflects the behavior in the metallic phase as opposed to the phenomenological underdamped model plotted in Fig. 2 [35].

In this Letter, we provide evidence that the continuous MIT observed in $NaOsO_3$ extends to a continuous evolution of the magnetic quasiparticle spectrum. The magnetic excitations at 300 K appear to be weakly Landau damped at all wave vectors, as a consequence of the emergent charge gap below the MIT. Meanwhile, at 450 K, these excitations become diffusive and can be successfully modeled within a weakly antiferromagnetic Fermi liquid picture. Such an approach naturally requires the presence of correlations in the high-temperature phase, which leads to a departure from mean-field behavior required for a pure Slater MIT. Therefore, we conclude that $NaOsO_3$ lies proximate to, but not within, the Slater limit.

A number of similarities can be drawn between the behavior of the magnetic excitations in $NaOsO_3$ and those observed for the cuprates and pnictides as a function of the carrier doping. The distinction in $NaOsO_3$ is that the continuous evolution of the magnetic quasiparticle spectra occurs within a single system, through tuning of the temperature alone. This is in contrast to the cuprates and pnictides, where measurements have to be performed on multiple systems with different doping levels, slightly different experimental conditions, and so forth. Hence, $NaOsO_3$ is an ideal system for testing theoretical predictions of the RIXS response as a function of the strength of electronic interaction. The results presented here (and in Ref. [26]) suggest a correspondence between the dynamic structure factor $S(\boldsymbol{Q}, \omega)$ and the RIXS cross section in the itinerant limit.

*j.vale@ucl.ac.uk
†caldersa@ornl.gov

[1] W. Witczak-Krempa, G. Chen, Y. B. Kim, and L. Balents, Annu. Rev. Condens. Matter Phys. **5,** 57 (2014).

[2] J. G. Rau, E. K.-H. Lee, and H.-Y. Kee, Annu. Rev. Condens. Matter Phys. **7,** 195 (2016).

[3] T. Moriya, *Spin Fluctuations in Itinerant Electron Magnetism*, Springer Series in Solid-State Sciences (Springer-Verlag, Berlin, 1985).

[4] M. Le Tacon, G. Ghiringhelli, J. Chaloupka, M. M. Sala, V. Hinkov, M. Haverkort, M. Minola, M. Bakr, K. Zhou, S. Blanco-Canosa, C. Monney, Y. T. Song, G. L. Sun, C. T. Lin, G. M. De Luca, M. Salluzzo, G. Khaliullin, T. Schmitt, L. Braicovich, and B. Keimer, Nat. Phys. **7,** 725 (2011).

[5] M. P. M. Dean, G. Dellea, R. S. Springell, F. Yakhou-Harris, K. Kummer, N. B. Brookes, X. Liu, Y.-J. Sun, J. Strle, T. Schmitt, L. Braicovich, G. Ghiringhelli, I. Boovi, and J. P. Hill, Nat. Mater. **12,** 1019 (2013).

[6] C. Monney, T. Schmitt, C. E. Matt, J. Mesot, V. N. Strocov, O. J. Lipscombe, S. M. Hayden, and J. Chang, Phys. Rev. B **93,** 075103 (2016).

[7] S. O. Diallo, V. P. Antropov, T. G. Perring, C. Broholm, J. J. Pulikkotil, N. Ni, S. L. Bud'ko, P. C. Canfield, A. Kreyssig, A. I. Goldman, and R. J. McQueeney, Phys. Rev. Lett. **102,** 187206 (2009).

[8] J. Zhao, D. Adroja, D.-X. Yao, R. Bewley, S. Li, X. Wang, G. Wu, X. Chen, J. Hu, and P. Dai, Nat. Phys. **5,** 555 (2009).

[9] K.-J. Zhou, Y.-B. Huang, C. Monney, X. Dai, V. N. Strocov, N.-L. Wang, Z.-G. Chen, C. Zhang, P. Dai, L. Patthey, J. van den Brink, H. Ding, and T. Schmitt, Nat. Commun. **4,** 1470 (2013).

[10] C. Wang, R. Zhang, F. Wang, H. Luo, L. P. Regnault, P. Dai, and Y. Li, Phys. Rev. X **3,** 041036 (2013).

[11] Z. Leong, W.-C. Lee, W. Lv, and P. Phillips, Phys. Rev. B **90,** 125158 (2014).

[12] P. Dai, Rev. Mod. Phys. **87,** 855 (2015).

[13] K. Matsuhira, M. Wakeshima, Y. Hinatsu, and S. Takagi, J. Phys. Soc. Jpn. **80,** 094701 (2011).

[14] M. Nakayama, T. Kondo, Z. Tian, J. J. Ishikawa, M. Halim, C. Bareille, W. Malaeb, K. Kuroda, T. Tomita, S. Ideta, K. Tanaka, M. Matsunami, S. Kimura, N. Inami, K. Ono, H. Kumigashira, L. Balents, S. Nakatsuji, and S. Shin, Phys. Rev. Lett. **117,** 056403 (2016).

[15] D. Mandrus, J. R. Thompson, R. Gaal, L. Forro, J. C. Bryan, B. C. Chakoumakos, L. M. Woods, B. C. Sales, R. S. Fishman, and V. Keppens, Phys. Rev. B **63,** 195104 (2001).

[16] W. J. Padilla, D. Mandrus, and D. N. Basov, Phys. Rev. B **66,** 035120 (2002).

[17] J. Yamaura, K. Ohgushi, H. Ohsumi, T. Hasegawa, I. Yamauchi, K. Sugimoto, S. Takeshita, A. Tokuda, M. Takata, M. Udagawa, M. Takigawa, H. Harima, T. Arima, and Z. Hiroi, Phys. Rev. Lett. **108,** 247205 (2012).

[18] Y. G. Shi, Y. F. Guo, S. Yu, M. Arai, A. A. Belik, A. Sato, K. Yamaura, E. Takayama-Muromachi, H. F. Tian, H. X. Yang, J. Q. Li, T. Varga, J. F. Mitchell, and S. Okamoto, Phys. Rev. B **80,** 161104 (2009).

[19] S. Calder, V. O. Garlea, D. F. McMorrow, M. D. Lumsden, M. B. Stone, J. C. Lang, J.-W. Kim, J. A. Schlueter, Y. G. Shi, K. Yamaura, Y. S. Sun, Y. Tsujimoto, and A. D. Christianson, Phys. Rev. Lett. **108,** 257209 (2012).

[20] Y. Du, X. Wan, L. Sheng, J. Dong, and S. Y. Savrasov, Phys. Rev. B **85**, 174424 (2012).

[21] M.-C. Jung, Y.-J. Song, K.-W. Lee, and W. E. Pickett, Phys. Rev. B **87**, 115119 (2013).

[22] I. L. Vecchio, A. Perucchi, P. Di Pietro, O. Limaj, U. Schade, Y. Sun, M. Arai, K. Yamaura, and S. Lupi, Sci. Rep. **3**, 2990 (2013).

[23] B. Kim, P. Liu, Z. Ergönenc, A. Toschi, S. Khmelevskyi, and C. Franchini, Phys. Rev. B **94**, 241113 (2016).

[24] S. Calder, J. H. Lee, M. B. Stone, M. D. Lumsden, J. C. Lang, M. Feygenson, Z. Zhao, J.-Q. Yan, Y. G. Shi, Y. S. Sun, Y. Tsujimoto, K. Yamaura, and A. D. Christianson, Nat. Commun. **6**, 8916 (2015).

[25] S. Calder, J. G. Vale, N. Bogdanov, C. Donnerer, D. Pincini, M. Moretti Sala, X. Liu, M. H. Upton, D. Casa, Y. G. Shi, Y. Tsujimoto, K. Yamaura, J. P. Hill, J. van den Brink, D. F. McMorrow, and A. D. Christianson, Phys. Rev. B **95**, 020413 (2017).

[26] J. G. Vale, S. Calder, C. Donnerer, D. Pincini, Y. G. Shi, Y. Tsujimoto, K. Yamaura, M. M. Sala, J. van den Brink, A. D. Christianson, and D. F. McMorrow, Phys. Rev. B **97**, 184429 (2018).

[27] M. W. Haverkort, Phys. Rev. Lett. **105**, 167404 (2010).

[28] C. J. Jia, E. A. Nowadnick, K. Wohlfeld, Y. F. Kung, C.-C. Chen, S. Johnston, T. Tohyama, B. Moritz, and T. P. Devereaux, Nat. Commun. **5**, 3314 (2014).

[29] B. J. Kim and G. Khaliullin, Phys. Rev. B **96**, 085108 (2017).

[30] Data for other momentum transfers are presented in Ref. [26].

[31] P. A. Fedders and P. C. Martin, Phys. Rev. **143**, 245 (1966).

[32] D. Inosov, J. Park, P. Bourges, D. Sun, Y. Sidis, A. Schneidewind, K. Hradil, D. Haug, C. Lin, B. Keimer, and V. Hinkov, Nat. Phys. **6**, 178 (2010).

[33] G. S. Tucker, R. M. Fernandes, D. K. Pratt, A. Thaler, N. Ni, K. Marty, A. D. Christianson, M. D. Lumsden, B. C. Sales, A. S. Sefat, S. L. Bud'ko, P. C. Canfield, A. Kreyssig, A. I. Goldman, and R. J. McQueeney, Phys. Rev. B **89**, 180503 (2014).

[34] S. O. Diallo, D. K. Pratt, R. M. Fernandes, W. Tian, J. L. Zarestky, M. Lumsden, T. G. Perring, C. L. Broholm, N. Ni, S. L. Bud'ko, P. C. Canfield, H.-F. Li, D. Vaknin, A. Kreyssig, A. I. Goldman, and R. J. McQueeney, Phys. Rev. B **81**, 214407 (2010).

[35] Further improvements in the quantitative agreement with the experimental data could likely be made by considering anisotropic spin fluctuations or the effect of finite momentum resolution of the spectrometer. However, there are insufficient data to perform this robustly.

[36] M. Moretti Sala, K. Martel, C. Henriquet, A. Al Zein, L. Simonelli, C. Sahle, H. Gonzalez, M.-C. Lagier, C. Ponchut, S. Huotari, R. Verbeni, M. Krisch, and G. Monaco, J. Synchrotron Rad. **25**, 580 (2018).